Over-barrier crossing in multidimensional tunneling

Thorsteinsson, Páll J.; Henriksen, Niels E.

Published in:
Chemical Physics Letters

Link to article, DOI:
10.1016/j.cplett.2021.139255

Publication date:
2022

Document Version
Publisher's PDF, also known as Version of record

Chemical Physics Letters 787 (2022) 139255

Contents lists available at ScienceDirect

Chemical Physics Letters

journal homepage: www.elsevier.com/locate/cplett

Over-barrier crossing in multidimensional tunneling

Páll J. Thorsteinsson, Niels E. Henriksen *

Department of Chemistry, Technical University of Denmark, Building 207, DK-2800 Kongens Lyngby, Denmark

ARTICLE INFO

Keywords:
Quantum dynamics
Multidimensional tunneling

ABSTRACT

Studies of the dissociative chemisorption of N_2 using two-dimensional empirical potential energy surfaces that differ by the position of the saddle point, all show high tunneling probabilities at energies well below the saddle-point energy of the reaction. This is highly unusual for a heavy-atom system and contradicted by one-dimensional analysis along the minimum-energy path. A mechanism of over-barrier crossing, related to the high-momentum tail of the vibrational wave function of N_2, is demonstrated. We analyze the two-dimensional wave-packet propagation and compares to the probability of having vibrational momenta that exceeds the value required to overcome the relevant barrier.

1. Introduction

It is well-known that tunneling plays an important role for chemical reactions involving light atoms like hydrogen. We study the quantum dynamics of tunneling for a model describing the dissociative chemisorption of N_2. This model, introduced by Kosloff and co-workers, described experimental results for the energy-resolved sticking coefficient of N_2 on catalytic metal surfaces (Ru(s) and Re(s) predominantly) [1–3]. The model, while being in qualitative agreement with molecular beam experiments, suggested a substantial tunneling effect for this heavy-atom system with transmission probabilities as high as $\mathcal{O}(10^{-4})$ at collision energies well below the saddle-point energy. The purpose of this Letter is to investigate the mechanism of this process with the aim of shedding light on the tunneling phenomenon beyond the one-dimensional description.

The model includes two-degrees of freedom of N_2, the inter-atomic bond length (r) and the distance of the molecules center of mass to the catalytic metal surface (z), with the bond axis being fixed parallel to the surface. An empirical potential energy surface is constructed with parameters chosen in order to comply with known experimental data. A full-dimensional description would include the four other degrees of freedom and hence any effects from surface corrugation leading to a distribution of barriers, along with any electronic degrees of freedom and interactions with surface phonons.

It should be noted that after the proposal of the above-mentioned model, full six-dimensional potential energy surfaces based on extensive DFT calculations have become available [4–6]. When highlighting the dependence on the r and z-coordinates, these potential energy surfaces for the interaction of N_2 with a catalytic surface are qualitatively similar to the empirical surface but includes of course the dependence on the orientation of N_2 as well as surface corrugation. Six-dimensional quantum calculations of the reaction probability suggested that tunneling is not playing any major role in the dissociative chemisorption of N_2 [4,7].

2. Methods and Results

The empirical potential energy surface (PES) is constructed from two diabatic surfaces modelling the precursor physisorbed state and the dissociative chemisorbed state [8,9]. In the following, we briefly summarize the procedure. The inter-atomic potential in the physisorbed state is described with a modified Morse potential, where the force constant is gradually weakened as the molecule approaches the surface by employing a smoothing function near the surface. The molecule-surface interaction is described with a weak-acting long-range dispersion potential [10,11]. In the chemisorbed state the individual nitrogen-atom interactions are modelled with a repulsive exponential potential, while the nitrogen-atom-surface interaction is modelled with a standard Morse potential. The two diabatic surfaces interact via an interaction potential, set at 7.5 kJ/mol at the minimum of the seam [1,12,13].

While the majority of the parameters are known experimentally a handful are unknown and thus remain free parameters, and can be used to achieve the desired PES topology. The barrier height is chosen such that it is similar to the result of the full DFT calculations, i.e., the classical barrier height remains fixed at 1.1 eV [4]. Given that the focus in this letter is on low-energy collisions, where tunneling is relevant, we

* Corresponding author.
E-mail address: neh@kemi.dtu.dk (N.E. Henriksen).

https://doi.org/10.1016/j.cplett.2021.139255
Received 4 October 2021; Received in revised form 18 November 2021; Accepted 21 November 2021
Available online 26 November 2021

study the dynamics solely on the lower adiabatic surface, as opposed to the non-adiabatic dynamics included previously by Kosloff and co-workers. This should have no appreciable effect on the final results as we do not expect non-adiabatic dynamics to play a role in low-energy simulations, as this mechanism was originally added to damp the reaction probability at high impact energies [14,9].

By varying the experimentally unknown parameters, we study three different topologies for this model with, *early*, *mixed* and *late* barrier types, respectively. The PES for the late-barrier system can be seen in Fig. 1. The potential along the one-dimensional reaction coordinate (s) for these three systems does not differ significantly and thus we consider a one-dimensional treatment for the late barrier system being representative of all systems. The imaginary frequency at the saddle point ($i1614\,\mathrm{cm}^{-1}$) is substantially higher than the imaginary frequency in the DFT result ($i409\,\mathrm{cm}^{-1}$), i.e., the barrier on the model potential is more narrow than the DFT result [4].

For reference we have calculated the one-dimensional minimum energy path (MEP) using the nudged elastic band method [15,16] with mass-scaled coordinates. Along with obtaining the reaction coordinate we also corrected for vibrational zero-point energy along the reaction coordinate using the reaction path hamiltonian method [17], obtaining the vibrational frequencies $\omega_\perp(s)$ orthogonal to the reaction coordinate. The zero-point energy corrected potential is then

$$V(s) = V_{\mathrm{MEP}}(s) + \hbar\omega_\perp(s)/2 \tag{1}$$

where $V_{\mathrm{MEP}}(s)$ is the potential along the MEP. By employing mass-scaled coordinates along the reaction coordinate we effectively eliminate any ambiguity regarding the mass associated with the reaction coordinate.

To that end we calculated the transmission probabilities using the semi-classical extended WKB method [18,19]

$$T_{\mathrm{WKB}}(E) = \left(1 + \exp\left[(2/\hbar)\int_a^b |p(s)|ds\right]\right)^{-1} \tag{2}$$

with $|p(s)| = \sqrt{2m(V(s)-E)}$ being the classical momentum and a and b are the classical turning points, where $V(a) = V(b) = E$. Transmission probabilities were calculated both for $V_{\mathrm{MEP}}(s)$ along the reaction coordinate and for $V(s)$ with the potential corrected for vibrational zero-point energy.

To further validate the results, we propagated a one-dimensional wave-packet along the reaction coordinate. A Gaussian wave-packet was chosen as the initial state mimicking a molecular beam,

$$\psi(s) = \left(2\pi(\Delta s)^2\right)^{-1/4}\exp\left(-\frac{(s-s_0)^2}{4(\Delta s)^2} - \frac{ip_0 s}{\hbar}\right) \tag{3}$$

where s_0 is the initial mean position (typically far removed, $s_0 \sim -15$ Å, from the top of the barrier, set as $s = 0$, since the wave function is very delocalized in coordinate space), p_0 is the initial mean momentum and Δs is the position uncertainty chosen such that the energy spread is very small ($\Delta E = 0.43$ meV). The numerical time-propagation according to the time-dependent Schrödinger equation was performed using the split-operator method and the FFT-method for the evaluation of the kinetic energy operator on a highly resolved grid (~ 10.000 grid-points) [20,21].

The results from the one-dimensional analysis are visualized in Fig. 2, showing good agreement between results from the WKB method and numerical wave-packet propagation. For the zero-point energy corrected potential, we use the late-barrier system in Fig. 1 where $\omega_\perp(s=0) = 304\,\mathrm{cm}^{-1}$. It is observed that the transmission probabilities for this potential are somewhat higher than for the $V_{\mathrm{MEP}}(s)$ potential. The low probabilities in Fig. 2 are in line with what one would expect from a heavy-atom system with a fairly narrow barrier. However, there remains a many orders of magnitude discrepancy between these transmission probabilities and the probabilities obtained on the full two-dimensional PES, depending on the position of the barrier, as can be seen in Fig. 3.

The two-dimensional propagation was performed on the three different PES's, differing in barrier positions, with the fixed classical barrier height

$$V_{\mathrm{MEP}}(s=0) - V_{\mathrm{MEP}}(s\to-\infty) = 1.1\ \mathrm{eV} \tag{4}$$

We chose a grid size of $(r,z) \sim 1024 \times 512$ and use again the split-operator as a propagator. The initial wave function is a product $\Psi(z,r) = \psi(z)\phi_0(r)$ between a Gaussian wave packet (same as in Eq. (3)) and the vibrational wave function $\phi_0(r)$. The vibrational wave function is approximated as the harmonic ground state,

$$\phi_0(r) = \left(2\pi(\Delta r)^2\right)^{-1/4}\exp\left(-\frac{(r-r_0)^2}{4(\Delta r)^2}\right) \tag{5}$$

where $r_0 = 1.1$ Å is the equilibrium bond length of N_2 and the position uncertainty is determined from the vibrational frequency $(\Delta r)^2 =$

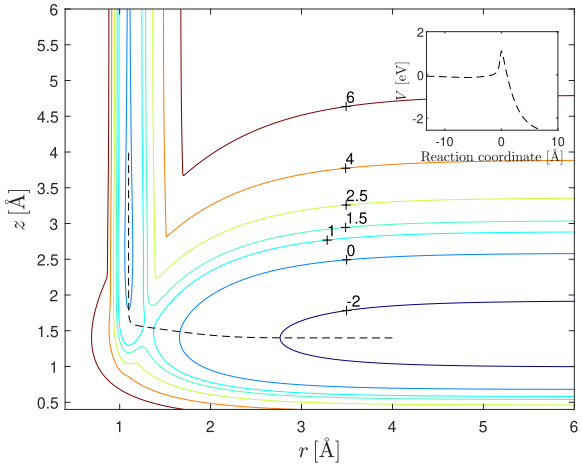

Fig. 1. Contours of the PES for a late-barrier system, all marked values are in eV. The dashed black line is the MEP of the system. The inset in the upper right corner shows the potential $V_{\mathrm{MEP}}(s)$ along the one-dimensional reaction coordinate.

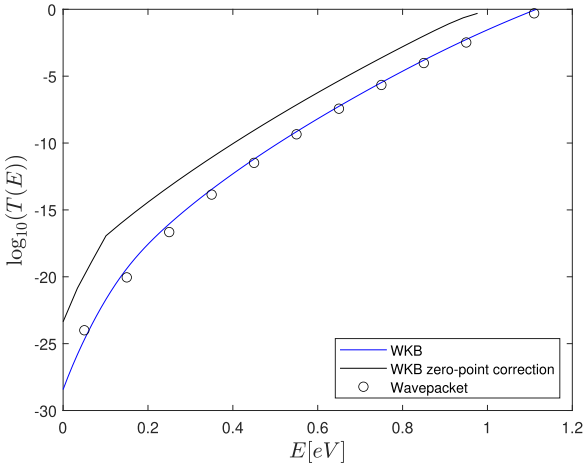

Fig. 2. Transmission probabilities $T(E)$ along the one-dimensional reaction coordinate. The solid black and blue line shows the transmission probability calculated with the semi-classical extended WKB theory, with and without the vibrational zero-point energy along the reaction coordinate, respectively. The circles show the transmitted norm from the wave-packet propagation along the reaction coordinate. The transmission probabilities are significantly lower than the results from the two-dimensional wave-packet propagation.

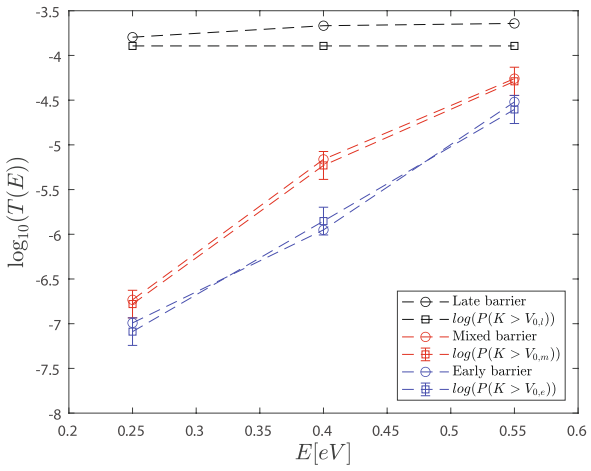

Fig. 3. Transmission probabilities from two-dimensional wave-packet propagation (circles) compared to the estimated probabilities (squares) from the high-momentum tail in the initial vibrational state according to Eq. (7) with $p_b = \sqrt{2\mu V_0}$, for the three systems. The observed barrier height V_0 is subject to some uncertainty (see text), the error bars correspond to an uncertainty of ± 0.05 eV.

$\hbar/(2\omega\mu)$, where the vibrational frequency $\omega = 2330\,\mathrm{cm}^{-1}$ and $\mu = 7$ amu is the reduced mass of nitrogen.

Fig. 3 shows transmission probabilities from the wave-packet propagation (circles) in the deep tunneling region, where the energies here are less than half of the barrier height. The transmission probabilities were obtained from the norm of the wave packet in the region where $r >$ 1.8 Å. It is observed that the transmission probabilities are roughly independent of the energy for the late-barrier case, whereas a strong energy dependence is observed for the other barrier types. These results agree overall with previously reported results for early and late barriers [1]. Furthermore, the transmission probabilities from the two-dimensional propagation are much larger than in the one-dimensional analysis as stated before. At the lowest energy of 0.25 eV, the difference is as large as $8-10$ orders of magnitude, depending on the position of the barrier, whereas the difference is about $3-4$ orders of magnitude at the heights energy of 0.55 eV. As such it is hard to rationalise the result as tunneling through the barrier, rather a mechanism to cross the barrier must be lost due to the reduction in dimensionality.

Fig. 4 shows a snapshot of the probability density for the late-barrier case. A logarithmic scale is used in order to visualize both high and extremely low values of the density. The snapshot is taken at the time where the density moving into the dissociation channel takes its maximum value (the contour levels are here around 10^{-5}). It is observed that the small fraction of the wave packet moving into the dissociation channel is in the neighbourhood of the MEP. Thus, the crossing is taking place in a region of the PES where the classical barrier height is ~ 1.1 eV. By observing the time-evolution of the probability density, it is seen that the predominant path in both the mixed-barrier system (see Fig. 5) and the early-barrier system (not shown) does not pass over the saddle point, rather the path taken is across a barrier, higher in potential than the saddle point. This amounts to a higher classical barrier and by observing where on the PES the peak of the transmitted wave crosses the barrier, an effective classical barrier height can be estimated in a straightforward manner.

We propose that the barrier crossing is related to the momentum spread in the initial vibrational state. N_2 possesses one of the strongest bonds in nature leading to an unusually localised bond in coordinate space and, of course, due to the uncertainty principle it means that N_2 is delocalized in momentum space, leading to a high-momentum tail. Representing the wave function in Eq. (5) in momentum space, the probability density is

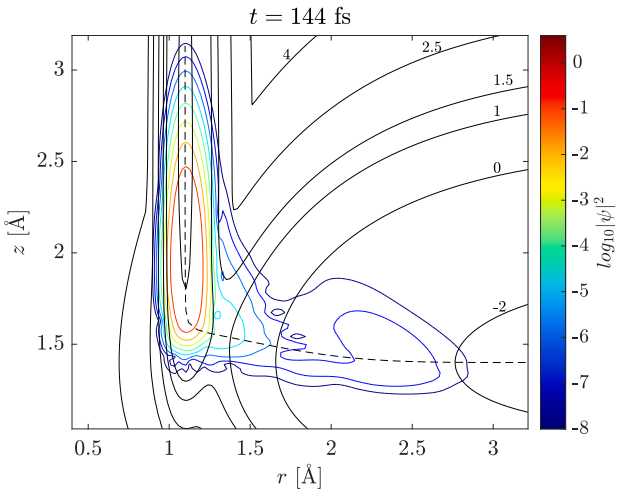

Fig. 4. Snapshot of the probability density for the late-barrier system at the climax of the barrier crossing (note logarithmic scale). The incident kinetic energy is 0.25 eV and the initial mean position is $z_0 = 4$ Å. The dashed black line is the MEP of the system while the solid black lines are contours of the PES, with all marked values in eV. In the case of the late barrier, the path taken is consistent with the MEP and thus the observed barrier height is ~ 1.1 eV.

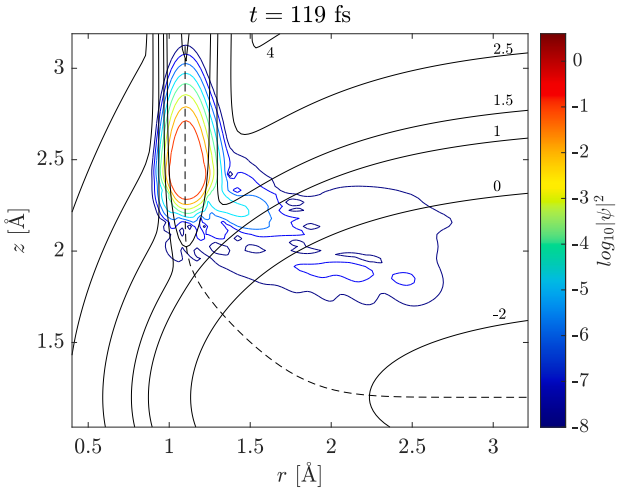

Fig. 5. Snapshot of the probability density for the mixed-barrier system at the climax of the barrier crossing (note logarithmic scale). The incident kinetic energy is 0.4 eV and the initial mean position is $z_0 = 4$ Å. The dashed black line is the MEP of the system while the solid black lines are contours of the PES, with all marked values in eV. In the case of the mixed barrier, the main path taken is not along the MEP, as a result the observed barrier height (~ 1.4 eV here) is higher than along the MEP.

$$|\widetilde{\phi}_0(p_r)|^2 = \sqrt{2(\Delta r)^2/(\pi\hbar^2)}\exp\left(-\frac{2(\Delta r)^2 p_r^2}{\hbar^2}\right) \tag{6}$$

The probability of finding momenta that exceeds a threshold value of p_b is then given by [14]

$$\begin{aligned} P(p_r > p_b) &= \int_{p_b}^{\infty} |\widetilde{\phi}_0(p_r)|^2 dp_r \\ &= (1/2)\mathrm{erfc}\left[\sqrt{2}\,p_b \Delta r \Big/ \hbar\right] \end{aligned} \tag{7}$$

where erfc is the complementary error function,

$$\mathrm{erfc}(x) = 1 - \frac{2}{\sqrt{\pi}} \int_0^x e^{-u^2} du \tag{8}$$

The classical kinetic energy required to pass a potential barrier V_0 is $K = p_b^2/(2\mu) = V_0$, corresponding to the momentum $p_b = \sqrt{2\mu V_0}$. That is, $P(K > V_0) = P(p_r > p_b)$ as in Eq. (7).

As shown in Fig. 3, the transmission probabilities are estimated with impressive accuracy according to Eq. (7) for $p_b = \sqrt{2\mu V_0}$, using the observed barrier heights V_0. In the results for the late barrier, we corrected for vibrational zero-point energies along the MEP, with $\omega_\perp(s = 0) = 304\,\mathrm{cm}^{-1}$, this gives $V_0 = 0.98$ eV. For the other barrier types, we used directly the observed barrier heights obtained as in Fig. 5. These barrier heights are, of course, subject to some uncertainty. By carefully selecting the snapshot where the density moving into the dissociation channel takes its maximum value and by zooming in on the relevant region, we estimate an uncertainty of $\pm$ 0.05 eV in the barrier height V_0.

This strongly suggests that the crossing is indeed due to the high-momentum tail in the initial vibrational state. While under most circumstances, without further discussion, this event would be classified as tunneling, it is not genuine dynamical tunneling through the barrier but an "apparent type" of tunneling. It is *over-barrier crossing*, specifically due to a high-momentum tail of a localized vibrational degree of freedom, allowing crossing of a barrier not predicted in one-dimensional analysis.

3. Discussion

It is well-known that transmission probabilities in the tunneling region restricted to the one-dimensional MEP can underestimate tunneling due to contributions from tunneling paths outside of the MEP [22,23].

We have demonstrated that tunneling in the two-dimensional reaction dynamics of dissociative chemisorption of N_2 can take place as over-barrier crossing, not predicted by one-dimensional MEP analysis. This is another case where tunneling estimates along the one-dimensional MEP will underestimate the true reaction probability. The mechanism is related to the very broad momentum distribution of the vibrational ground state of the N_2 molecule and the fact that the employed model potential energy surface to a large extend preserves this distribution right until the barrier crossing takes place. The idea that the high-momentum tail of an initial vibrational state can contribute to barrier crossing in the tunneling regime has been suggested before (see, e.g., Refs. [14,24]) but the validity of this proposition is now shown very explicitly in this work, for three different positions of the saddle point. Reactions involving strongly localized bonds like in N_2 seems to be good candidates for tunneling via over-barrier crossing.

Fig. 3 shows that the largest transmission probabilities are obtained for the late-barrier case. To that end it is interesting to note that the work of Polanyi (and others) [25,26] has shown that vibrational (compared to translational) energy is most effective for passage over a late barrier. This observation has its origins in a classical description of molecular reaction dynamics, i.e., at total energies above the saddle-point energy. Our findings are also related to the vibrational degree of freedom. However, what we observe in the tunneling region is a pure quantum effect; we have passage over the barrier due to the momentum uncertainty associated with the vibrational state. The destinction between vibrational and translational energy is not included in present (one-dimensional) descriptions of tunneling.

We note in passing that the position of the saddle-point in the six-dimensional DFT calculation of dissociative chemisorption of N_2 is much "later" ($r \sim 2$ Å), i.e., further into the dissociative product channel than we could generate by varying the experimentally unknown parameters in the model potential. If the dynamics following the change in the PES from the entrance channel to the low-frequency region around the saddle point is adiabatic, the high-momentum components will disappear. This might explain why over-barrier tunneling is not playing any role on this potential energy surface where small transmission probabilities $\mathcal{O}(10^{-5})$ are already found at an energy of 0.1 eV below the saddle-point energy [4]. The transmission probability can in this case be well explained by the low values obtained from one-dimensional tunneling along the minimum-energy path.

Finally, to summarize, a note on the title of this Letter. Clearly, if tunneling is defined as propagation through a potential barrier, there is a contradiction in the wording. We find transmission (reaction) at total energies well below the barrier (saddle-point) energy. This is a tunneling phenomenon, according to a general definition of tunneling, where it means propagation/penetration into regions of configuration space that are not accessible according to classical mechanics (at the same total energy). In one dimension, this definition coincides with the "textbook" definition of a wave function that propagates through a potential barrier.

Declaration of Competing Interest

The authors declare that they have no known competing financial interests or personal relationships that could have appeared to influence the work reported in this paper.

References

[1] G. Haase, M. Asscher, R. Kosloff, The dissociative chemisorption dynamics of n2 on catalytic metal surfaces: A quantum-mechanical tunneling mechanism, J. Chem. Phys. 90 (6) (1989) 3346–3355, https://doi.org/10.1063/1.456666 [Online]. Available:.

[2] L. Romm, G. Katz, R. Kosloff, M. Asscher, Dissociative chemisorption of n2 on ru (001) enhanced by vibrational and kinetic energy: Molecular beam experiments and quantum mechanical calculations, J. Phys. Chem. B 101 (12) (1997) 2213–2217, https://doi.org/10.1021/jp962599o [Online]. Available:.

[3] G. Katz, R. Kosloff, Temperature dependence of nitrogen dissociation on metal surfaces, J. Chem. Phys. 103 (21) (1995) 9475–9481, https://doi.org/10.1063/1.470008 [Online]. Available:.

[4] R. van Harrevelt, K. Honkala, J. Nørskov, U. Manthe, The reaction rate for dissociative adsorption of n2 on stepped ru(0001): Six-dimensional quantum calculations, J. Chem. Phys. 122 (11) (2005) 234702, https://doi.org/10.1063/1.1927513 [Online]. Available:.

[5] K. Shakouri, J. Behler, J. Meyer, and G.-J. Kroes, "Analysis of energy dissipation channels in a benchmark system of activated dissociation: N2 on ru(0001)," The Journal of Physical Chemistry C, vol. 122, no. 41, pp. 23 470–23 480, 2018. [Online]. Available: 10.1021/acs.jpcc.8b06729.

[6] P. Spiering, K. Shakouri, J. Behler, G.-J. Kroes, and J. Meyer, "Orbital-dependent electronic friction significantly affects the description of reactive scattering of n2 from ru(0001)," The Journal of Physical Chemistry Letters, vol. 10, no. 11, pp. 2957–2962, 2019, pMID: 31088059. [Online]. Available: 10.1021/acs.jpclett.9b00523.

[7] S. Dahl, A. Logadottir, R.C. Egeberg, J.H. Larsen, I. Chorkendorff, E. Törnqvist, J. K. Nørskov, Role of steps in n_2 activation on ru(0001), Phys. Rev. Lett. 83 (Aug 1999) 1814–1817 [Online]. Available: https://link.aps.org/doi/10.1103/PhysRevLett.83.1814.

[8] E. Por, G. Haase, O. Citri, R. Kosloff, M. Asscher, Effect of molecular energy content on the dissociative chemisorption of n2 on re(0001), Chem. Phys. Lett. 186 (6) (1991) 553–560 [Online]. Available: https://www.sciencedirect.com/science/article/pii/000926149190466M.

[9] G.D. Billing, A. Guldberg, N.E. Henriksen, F.Y. Hansen, Dissociative chemisorption of n2 on rhenium: Dynamics at low impact energies, Chem. Phys. 147 (1) (1990) 1–11 [Online]. Available: https://www.sciencedirect.com/science/article/pii/030101049085015O.

[10] K.T. Tang, J.P. Toennies, An improved simple model for the van der waals potential based on universal damping functions for the dispersion coefficients, J. Chem. Phys. 80 (8) (1984) 3726–3741, https://doi.org/10.1063/1.447150 [Online]. Available:.

[11] M. Asscher, G. Haase, and R. Kosloff, "Tunneling mechanism for the dissociative chemisorption of n2 on metal surfaces," Vacuum, vol. 41, no. 1, pp. 269–271, 1990, surface Science Section. [Online]. Available: https://www.sciencedirect.com/science/article/pii/0042207X9090331R.

[12] N.E. Henriksen, G.D. Billing, F.Y. Hansen, Dissociative chemisorption of n2 on rhenium: Dynamics at high impact energies, Surf. Sci. 227 (3) (1990) 224–236 [Online]. Available: https://www.sciencedirect.com/science/article/pii/S003960280580010X.

[13] F.Y. Hansen, N.E. Henriksen, G.D. Billing, New insight in the microscopic mechanism of the catalytic synthesis of ammonia, Surf. Sci. 324 (1) (1995) 55–68 [Online]. Available: https://www.sciencedirect.com/science/article/pii/0039602894006342.

[14] N.E. Henriksen, F.Y. Hansen, and G.D. Billing, "Apparent tunneling in chemical reactions," Chemical Physics Letters, vol. 330, no. 139, 2000.

[15] G. Henkelman and H. Jónsson, "Improved tangent estimate in the nudged elastic band method for finding minimum energy paths and saddle points," Journal of Chemical Physics, vol. 113, no. 9978, 2000.
[16] G. Henkelman, B. Uberuaga, and H. Jónsson, "A climbing image nudged elastic band method for finding saddle points and minimum energy paths," Journal of Chemical Physics, vol. 113, no. 22, 2000.
[17] W. Miller, N. Handy, and J. Adams, "Reaction path hamiltonian for polyatomic molecules," Journal of chemical physics, vol. 72, no. 99, 1980.
[18] N.E. Henriksen, F.Y. Hansen, Theories of Molecular Reaction Dynamics, 2nd ed., Oxford University Press, 2018.
[19] M. Razavy, Quantum Theory of tunneling, 2nd ed., World Scientific, 2013.
[20] M. Feit, J. Fleck, A. Steiger, Solution of the schrödinger equation by a spectral method, J. Comput. Phys. 47 (1982) 412.
[21] R. Kosloff, Time dependent methods in molecular dynamics, The Journal of Physical Chemistry 92 (1988) 2087.
[22] D.G. Truhlar, M.S. Gordon, From force fields to dynamics: Classical and quantal paths, Science 249 (4968) (1990) 491–498.
[23] A. Fernandez-Ramos, D.G. Truhlar, Improved algorithm for corner-cutting tunneling calculations, J. Chem. Phys. 114 (4) (2001) 1491–1496.
[24] H.-W. Lee, T. George, Wigner phase-space description above and below the classical threshold for the h + h2 reaction, J. Chem. Phys. 84 (11) (1986) 6247.
[25] J.C. Polanyi, Some concepts in reaction dynamics, Acc. Chem. Res. 5 (1972) 161.
[26] Z. Zhang, Y. Zhou, D. Zhang, J.M. Bowman, Theoretical study of the validity of the polanyi rules for the late-barrier cl+chd3 reaction, Journal of Physical Chemistry Letters 3 (2012) 3416.